Original Article

Trichosanthin inhibits cell growth and metastasis by promoting pyroptosis in non-small cell lung cancer

Yan Tan[1], Junyu Xiang[2,3], Zixian Huang[2,3], Lin Wang[2,3], Yiling Huang[2,3]

[1]Department of Pulmonary and Critical Care Medicine, the First People's Hospital of Yunnan Province (The Affiliated Hospital of Kunming University of Science and Technology), Kunming, China; [2]Key Laboratory of Tumor Microenvironment and Immunotherapy, China Three Gorges University, Yichang, China; [3]Department of Pathology, Medical College of China Three Gorges University, Yichang, China

Contributions: (I) Conception and design: Y Tan, Y Huang; (II) Administrative support: L Wang, Y Huang; (III) Provision of study materials or patients: Y Tan, J Xiang; (IV) Collection and assembly of data: Y Tan, J Xiang, Z Huang, L Wang; (V) Data analysis and interpretation: Z Huang, L Wang; (VI) Manuscript writing: All authors; (VII) Final approval of manuscript: All authors.

Correspondence to: Yiling Huang. Department of Pathology, Medical College of China Three Gorges University, 8 DaXue Road, Yichang 443002, China. Email: HuangylTG@163.com.

Background: A number of studies have demonstrated that trichosanthin (TCS) can induce apoptosis in numerous types of tumor cell lines. However, whether TCS can induce pyroptosis has not yet been reported. This study aimed to investigate the role of TCS and its inhibitory effect on tumor growth by modulating pyroptosis in non-small cell lung cancer (NSCLC).

Methods: Effects of different concentrations of TCS on the cell viability, proliferation, migration and invasion of NSCLC were detected by Cell Counting Kit-8 (CCK-8), colony formation, migration, and invasion assays. Immunofluorescence was used to detect the effect of TCS on the expression of pyroptosis marker protein gasdermin-D (GSDMD)-N in A549 cells. A tumor xenograft animal model was established by injecting A549 cells into nude mice.

Results: In the present study, we found that TCS significantly inhibited the proliferation, migration, and invasion of A549 cells in a concentration-dependent manner. In addition, TCS at a high concentration (40 μg/mL) significantly promoted the expression of pyroptosis-related proteins [GSDMD-N, NLR family pyrin domain containing 3 (NLRP3), apoptosis-associated speck-like protein containing a CARD (ASC), caspase-1, and GSDMD], which showed an inhibitory effect on the pyroptosis of A549 cells. Additionally, we found that necrosulfonamide (NSA) significantly reversed the inhibitory effect of high concentrations of TCS on the pyroptosis of A549 cells. The in vivo experiments showed that TCS effectively reduced the tumor volume and inhibited the expression of Ki-67, whereas it increased the expression of GSDMD-N.

Conclusions: Taken together, these results indicated that TCS could inhibit the progression of NSCLC by promoting pyroptosis. These findings provide further information on the possible underlying mechanism of TCS in the treatment of NSCLC.

Keywords: Trichosanthin (TCS); non-small cell lung cancer (NSCLC); pyroptosis; migration; invasion

Submitted Jan 17, 2022. Accepted for publication Apr 11, 2022.
doi: 10.21037/jtd-22-282
View this article at: https://dx.doi.org/10.21037/jtd-22-282

Introduction

Non-small cell lung cancer (NSCLC) is a type of malignant tumor with high morbidity and mortality worldwide (1,2). Although NSCLC treatment has greatly improved, the 5-year survival rate remains less than 20% (3). Studies have revealed that the malignant proliferation and metastasis of cancer cells are the primary obstacles to improving the prognosis of patients (4,5). Therefore, studying the molecular mechanism of NSCLC proliferation and metastasis and developing more efficient therapeutic drugs

have become important strategies for treating NSCLC.

Cell death can be subdivided into different types: apoptosis, autophagy, programmed necrosis, and atypical death. Among these, apoptosis refers to the programmed death of cells that have received internal and external death signals. Many studies have shown that apoptosis plays an essential role in the antitumor mechanism of various drugs (6,7). Pyroptosis is a newly discovered type of programmed cell death that has become a focus of attention in recent years. In the early stages of research, it was initially considered to be apoptosis. Pyroptosis is a particular type of programmed death accompanied by the infiltration of a large number of inflammatory factors (8). The activation of pyroptosis mainly depends on the regulation of caspase-1, while the activation of caspase-1 is controlled by inflammasomes (9). Compared with apoptosis, there are few studies on pyroptosis in NSCLC. Previous study has demonstrated that NSCLC cells are extremely prone to autoimmune and inflammatory responses (10). Furthermore, a higher systemic level of inflammatory cytokines is significantly related to the poor prognosis of patients with NSCLC (11). Therefore, the present study hypothesized that pyroptosis, which is closely associated with inflammation, is involved in the progression of NSCLC.

Trichosanthin (TCS) is a single-chain ribosome-inactivating protein extracted from the root tuber of *Trichosanthes kirilowii* with a molecular weight of 27 kDa. It is reported that TCS has a variety of pharmacological uses, including the treatment of ectopic pregnancy and different types of tumors (such as choriocarcinoma) (12). In previous years, TCS was found to inhibit tumor progression by inducing apoptosis (13). Fang *et al.* (14) reported that TCS inhibits the proliferation of breast cancer cells by promoting apoptosis. Zhang *et al.* (15) demonstrated that TCS could significantly inhibit cancer progression by promoting the apoptosis of human choriocarcinoma cells. Besides cell apoptosis, TCS has been found to promote autophagy by activating the NF-κB/p53 pathway and enhancing the production of reactive oxygen species (ROS), which is the key substance involved in pyroptosis (16). In addition, TCS has shown promising antitumor efficacy in the treatment of NSCLC (17). TCS has been shown to enhance drug-sensitivity in NSCLC (17,18). TCS has been proved to exert inhibitory effects on different types of tumors including NSCLC, but whether the effects of TCS on NSCLC are associated with pyroptosis was still unclear. Thus, we further explored the mechanism of TCS in NSCLC.

In the present study, we aimed to explore the effects of TCS in NSCLC cells and its potential mechanism. We hypothesized that TCS could inhibit the progression of NSCLC by inducing pyroptosis *in vivo* and *in vitro*. We elucidated the antitumor effect of TCS from the perspective of pyroptosis, which may provide a novel fundamental insight into how TCS acts on NSCLC. We present the following article in accordance with the ARRIVE reporting checklist (available at https://jtd.amegroups.com/article/view/10.21037/jtd-22-282/rc).

Methods

Cell culture

Human bronchial epithelial (HBE) cells and three types of NSCLC cells (NCI-H1299, NCI-H1650, and A549) were purchased from The Shanghai Laboratory Animal Center of the Chinese Academy of Sciences (CAS). These cells were cultured in RPMI-1640 medium (Lonza Group, Ltd., Basel, Switzerland) containing 10% FBS, 100 U/mg penicillin, and 100 μg/mL streptomycin in a 5% CO_2 incubator at 37 ℃. Following detachment with trypsin, cells were passaged. Cells in the logarithmic phase were collected for follow-up assays. To explore the effects of TCS on NSCLC, different doses of TCS (10, 20, 40 and 60 μg/mL) were added into A549 cells.

Cell Counting Kit-8 (CCK-8) assay

Cell viability was detected using a CCK-8 assay. Cells were inoculated on 96-well plates at a density of 2×10^3 cells/well and treated with different doses of TCS (purchased from Professor Yanfa Meng from Sichuan University) for 24 and 48 h. A total of 10 μL CCK-8 solution was added to each well, and the culture was continued for an additional 2 h. The absorbance of each well was measured at 450 nm wavelength using a microplate reader (Synergy 2 Multi-Mode Microplate Reader; BioTek Instruments, Inc., Winooski, VT, USA).

Colony formation assay

Cells were inoculated in 6-well plates at a density of 4×10^2 cells/well for 14 days. Subsequently, the cells were fixed with 70% ethanol and then stained with 0.05% crystal violet for 20 min. The number of colonies formed

(>50 cells/colony) was counted under an Olympus BX40 light microscope (Olympus Corporation, Tokyo, Japan).

Wound healing assay

Cell migration was detected via a wound healing assay. Cells were inoculated in 12-well plates at a density of 2×10^4 cells/well. When confluency reached 90%, a standardized wound was created on the board surface with a 200-μL sterile pipette tip. Cells were imaged under an Olympus BX40 light microscope (Olympus Corporation) at 0 and 24 h.

Transwell assay

A Transwell assay was performed to determine cell invasion. Cells in the logarithmic growth phase (3×10^4 cells) were cultured in the top chamber of the Matrigel-coated invasion chambers (BD Biosciences, East Rutherford, NJ, USA) filled with serum-free DMEM/F12. The DMEM/F12 medium containing 10% FBS was added to the lower chamber. After 24 h of culture, cells were fixed with 80% ethanol for 30 min and stained with 0.1% crystal violet solution for 5 min. The stained cells were observed under an inverted microscope (Leica Microsystems, Inc., Shanghai, China).

Immunofluorescence analysis

Cells were fixed with acetone for 20 min and then incubated with 3% H_2O_2 at room temperature in the dark for 10 min. Afterward, the sections were incubated with goat serum at 37 ℃ for 10 min to block non-specific binding. The slices were incubated with primary antibodies against gasdermin-D (GSDMD)-N (1:1,000; cat. no. ab215203; Abcam, Cambridge, UK) and ROS (1:500; cat. no. ab238535; Abcam) overnight. Next, the slices were co-incubated with a PE-labeled secondary antibody for 2 h.

Immunohistochemistry

Tissue sections (4 μm) were fixed with 4% paraformaldehyde for 24 h and then embedded in paraffin for the following experiments. The sections were deparaffinized in xylene for 20 min and then washed with deionized water for 5 min. Then, the sections were treated with 10 nM citrate buffer and subsequently incubated with primary antibodies against Ki67 (1:1,000; cat. no. ab15580; Abcam) and GSDMD-N (cat. no. ab215203; Abcam). These slices were then incubated with the corresponding secondary antibody. Sections were observed and imaged under an inverted microscope (Leica Microsystems, Inc.).

Animal experiments

The present study was performed under a project license (No. YYLH017) granted by the Animal Care and Use Committee of The First People's Hospital of Yunnan Province (Kunming, China) and conducted in accordance with Chinese legislation regarding animal experiments. A total of 20 male BALB/c nude mice were purchased from the Nanjing Qinglongshan Animal Breeding Center (Nanjing, China) and kept in specific pathogen-free conditions with light/dark cycles of 12 h, 60% humidity, 23±3 ℃, and free access to water. The mice were randomly divided into two groups (n=10): a control group and a TCS group. Briefly, the mice were anesthetized with an intraperitoneal injection of pentobarbital (50 mg/kg). No signs of peritonitis, pain, or discomfort were observed after anesthesia. A549 (4×10^5) cells were subcutaneously injected into the nude mice. The TCS group received an additional intraperitoneal injection with 5 mg/kg TCS for 2 days, and the control group was injected intraperitoneally with the same volume of saline. The tumor volume and body weight of the mice were observed every day, and the tumor volume was recorded for a total of 14 days (the maximum tumor size did not exceed 1,000 mm^3). After the mice were euthanized by cervical dislocation, the tumor tissues were harvested and stored at –80 ℃ for further assays.

Western blot analysis

Total RNA was extracted from the cells using a RIPA buffer (cat. no. P0013B; Beyotime Institute of Biotechnology, Shanghai, China). The protein concentration was detected using a BCA protein quantitative kit (cat. no. P0012; Beyotime Institute of Biotechnology). The protein (20 μg) was separated with 10% SDS-PAGE and subsequently transferred to a PVDF membrane (cat. no. FFP30; Beyotime Institute of Biotechnology). The membranes were blocked with 5% skimmed milk for 30 min and incubated with primary antibodies (1:1,000) against NLR family pyrin domain containing 3 (NLRP3; cat. no. ab263899; Abcam), apoptosis-associated speck-like protein containing a CARD (ASC; cat. No. ab151700; Abcam), caspase-1 (cat. no. ab179515; Abcam), GSDMD (cat. no. ab219800; Abcam) and GAPDH (cat. no. ab2433; Abcam) overnight at 4 ℃, and then with the corresponding

horseradish peroxidase (HRP)-conjugated secondary antibodies at 37 ℃ for 2 h at appropriate dilutions. An ECL Plus kit (cat. no. P0018; Beyotime Institute of Biotechnology) was used to visualize the protein bands.

Statistical analysis

Data were analyzed using GraphPad Prism 7 (GraphPad Software, Inc., San Diego, CA, USA). The data are expressed as the mean ± standard deviation (SD). Student's *t*-test was used to compare the two groups. The comparison among multiple groups was determined using a one-way analysis of variance (ANOVA). A P value <0.05 was considered to indicate a statistically significant difference.

Results

TCS inhibited the proliferation, invasion, and migration of A549 cells

The effects of TCS on the viability, proliferation, migration, and invasion of NSCLC cells were detected by CCK-8, colony formation, wound healing, and Transwell assays, respectively. First, as shown in *Figure 1A*, TCS significantly inhibited the viability of NSCLC cells (NCI-H1299, A549, and NCI-H1650) compared with the HBE cells. TCS exerted the strongest inhibitory effect on the activity of A549 cells. Therefore, A549 cells were used in the follow-up experiments. The effects of different concentrations of TCS (10, 20, and 40 μg/mL) on the activity of A549 cells were detected via a CCK-8 assay. The CCK-8 assay results showed that TCS inhibited the activity of A549 cells in a concentration-dependent manner (*Figure 1B*). The colony formation assay results showed that, compared with the control group, TCS reduced the number of colonies of A549 cells in a concentration-dependent manner (*Figure 1C*). In addition, as shown in *Figure 1D-1G*, the wound healing and Transwell assays results showed that TCS suppressed the migration and invasion of A549 cells in a concentration-dependent manner compared with the control group.

TCS induced pyroptosis of A549 cells

Next, the expression of pyroptosis-related proteins was detected by immunofluorescence and western blotting. As shown in *Figure 2A,2B*, the immunofluorescence results showed that TCS promoted the expression of GSDMD-N and the level of ROS in a concentration-dependent manner compared with the control group. In addition, western blot results showed that, compared with the control group, TCS increased the expression of pyroptosis-related proteins, including NLRP3, ASC, caspase-1, and GSDMD, in a concentration-dependent manner. Overall, these results indicated that TCS effectively activated pyroptosis in A549 cells (*Figure 2C*).

TCS suppressed the proliferation, migration, and invasion of A549 cells by promoting pyroptosis

Necrosulfonamide (NSA), a pyroptosis inhibitor, was used to detect the effect of TCS on the activity of A549 cells to further determine whether TCS inhibited the activity of A549 cells by pyroptosis. As shown in *Figure 3A,3B*, NSA significantly inhibited the promotion of the GSDMD-N protein in A549 cells treated with TCS (40 μg/mL). As shown in *Figure 3C,3D*, results of the CCK-8 and colony formation assays showed that NSA reduced the inhibitory effect of TCS on the activity and proliferation of A549 cells. In addition, similar results were found in the wound healing and Transwell assays. As shown in *Figure 3E-3H*, NSA effectively alleviated the inhibitory effect of TCS on the migration and invasion of A549 cells.

TCS inhibited tumor growth in mice

Finally, the effect of TCS on tumor growth was detected by animal experiments (n=10). Compared with the control group, TCS significantly inhibited the size and volume of the tumor, as shown in *Figure 4A-4D*. In addition, compared with the control group, TCS significantly decreased the expression of Ki67 and increased the expression of GSDMD-N in tumor tissues. These results were consistent with the *in vitro* TCS experiments (*Figure 4E,4F*).

Discussion

The occurrence and development of NSCLC is a complex process that involves the dysregulation of multiple genes and signaling pathways. To date, the pathogenesis of NSCLC remains unknown. At present, most of the drugs for NSCLC are chemotherapeutic drugs that only kill rapidly proliferating tumor cells, thus the drug resistance of NSCLC cells affects the efficacy of chemotherapy. Compared with traditional chemotherapy drugs, traditional Chinese medicines have multiple advantages, including high

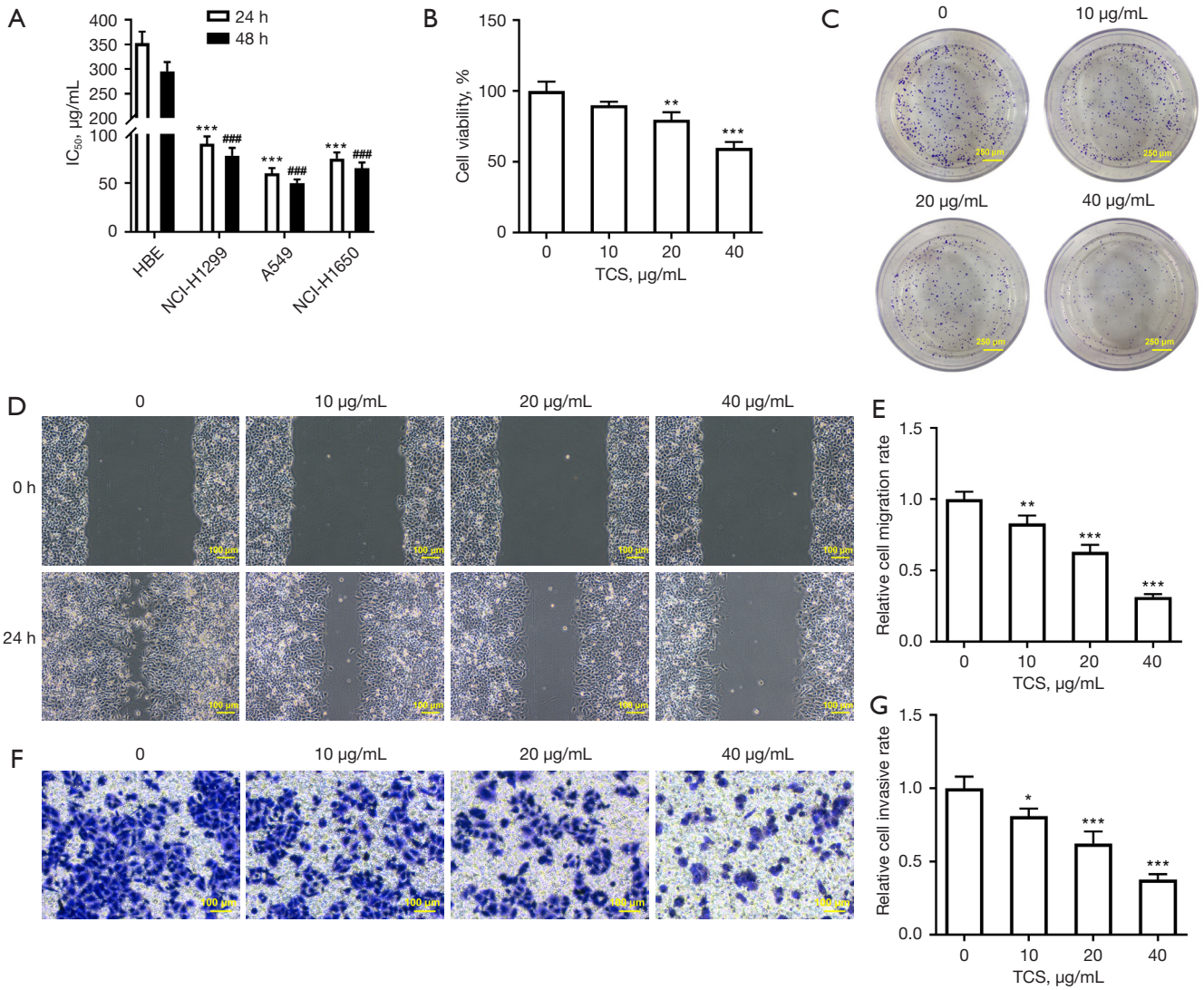

Figure 1 TCS inhibits the proliferation, invasion, and migration of A549 cells. (A) CCK-8 is performed to determine the effect of TCS on the activity of HBE cells and three types of NSCLC cells (NCI-H1299, NCI-H1650, and A549) at 24 and 48 h, respectively. ***P<0.001 *vs.* 24 h; ###P<0.001 *vs.* 48 h. (B) CCK-8 detects the effect of different concentrations of TCS (0, 10, 20, and 40 μg/mL) on the activity of A549 cells. **P<0.01 and ***P<0.001 *vs.* 0 μg/mL. (C) Colony formation assay detects the effect of different concentrations of TCS (0, 10, 20, and 40 μg/mL) on the proliferation of A549 cells, which was stained with 0.05% crystal violet. (D,E) Wound healing assay detects the effect of different concentrations of TCS (0, 10, 20, and 40 μg/mL) on the migration of A549 cells, which was observed by a light microscope. **P<0.01 and ***P<0.001 *vs.* 0 μg/mL. (F,G) Transwell assay detects the effect of different concentrations of TCS (0, 10, 20, and 40 μg/mL) on the invasion of A549 cells, which was stained with 0.1% crystal violet. *P<0.05 and ***P<0.001 *vs.* 0 μg/mL. IC_{50}, half maximal inhibitory concentration; HBE, human bronchial epithelial; TCS, trichosanthin; CCK-8, Cell Counting Kit-8; NSCLC, non-small cell lung cancer.

efficiency, low toxicity, and multiple targets of action in the field of antitumor research (19). Among them, TCS has become a research hotspot due to its potential antitumor activity. Several studies have shown that TCS can inhibit the activity of various tumor cells by inducing pyroptosis (12,20). However, to the best of our knowledge, no study has shown whether TCS can affect the activity of tumor cells by inducing pyroptosis. In the present study, TCS significantly inhibited the proliferation, migration, and invasion of A549 cells in a concentration-dependent manner. In addition,

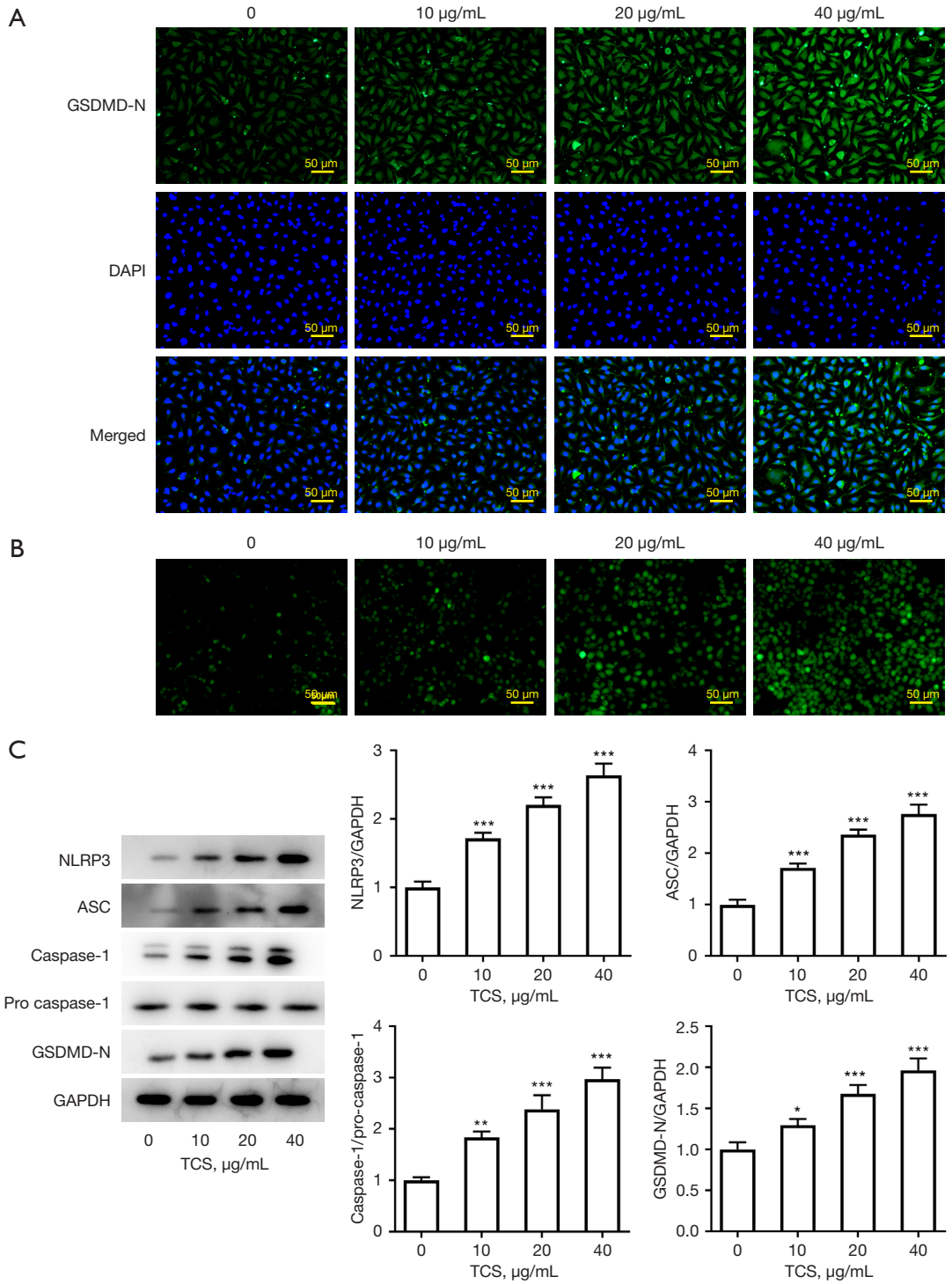

Figure 2 TCS induces pyroptosis of A549 cells. (A) Immunofluorescence determines the effect of different concentrations of TCS (0, 10, 20, and 40 μg/mL) on the expression of GSDMD-N. (B) Immunofluorescence determines the effect of different concentrations of TCS (0, 10, 20, and 40 μg/mL) on the ROS levels. (C) Western blotting measures the effect of different concentrations of TCS (0, 10, 20, and 40 μg/mL) on the pyroptosis-related proteins (NLRP3, ASC, caspase-1, pro caspase-1, GSDMD-N and GAPDH). *P<0.05, **P<0.01, and ***P<0.001 *vs.* 0 μg/mL. GSDMD, gasdermin-D; DAPI, 4',6-diamidino-2-phenylindole; NLRP3, NLR family pyrin domain containing 3; ASC, apoptosis-associated speck-like protein containing a CARD; TCS, trichosanthin; ROS, reactive oxygen species.

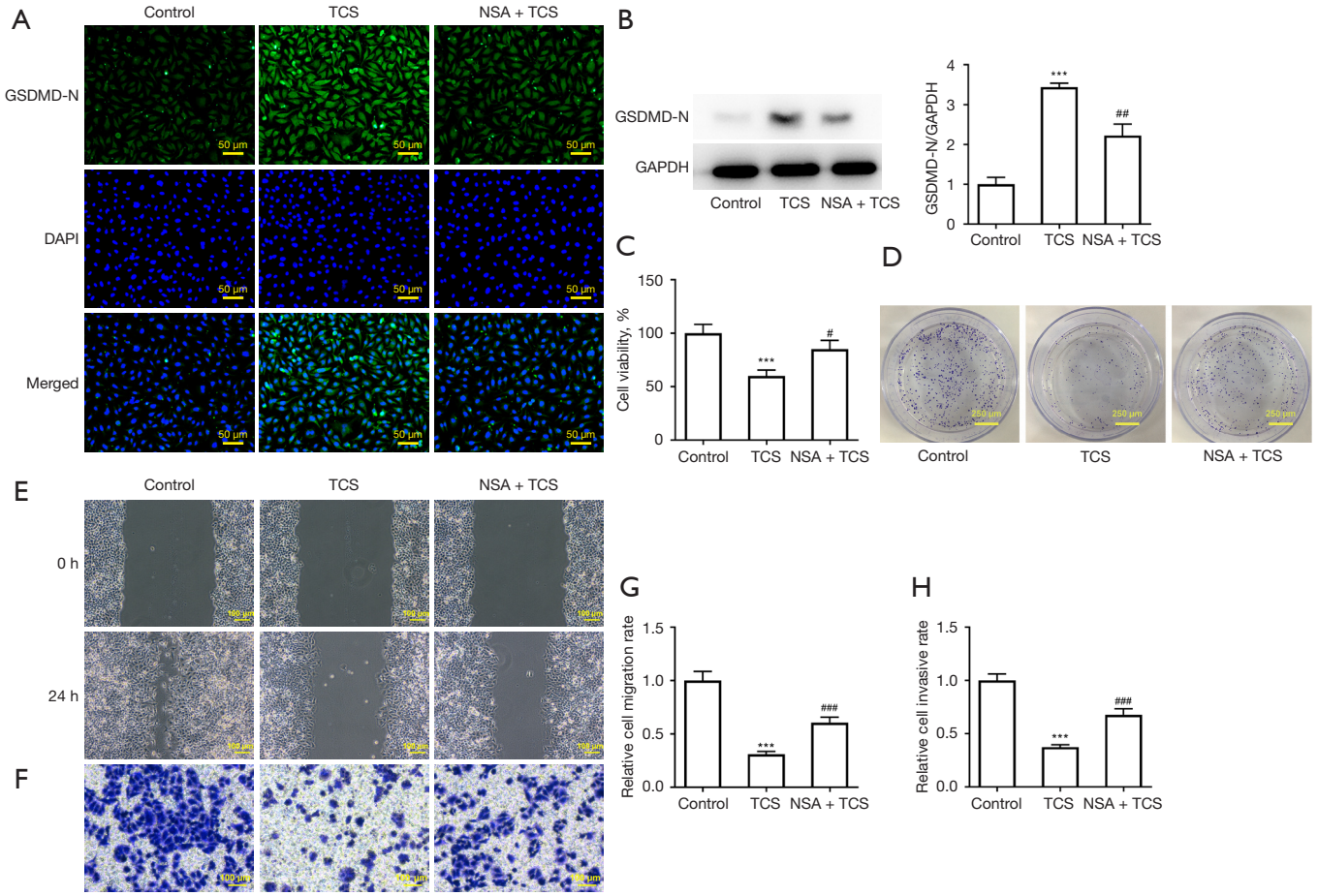

Figure 3 TCS suppresses the proliferation, migration, and invasion of A549 cells by promoting pyroptosis. (A) Immunofluorescence determines the effect of NSA on the expression of GSDMD-N. (B) Western blotting determines the effect of NSA on the expression of GSDMD-N. (C) CCK-8 detects the effect of NSA on the activity of A549 cells. (D) Colony formation assay detects the effect of NSA on the proliferation of A549 cells, which was stained with 0.05% crystal violet. (E-H) Wound healing and Transwell assays detect the effect of NSA on the migration and invasion of A549 cells, respectively. Wound healing assay was observed by a light microscope. Transwell assay was performed with staining with 0.1% crystal violet. ***P<0.001 *vs.* control; $^{\#}$P<0.05, $^{\#\#}$P<0.01, and $^{\#\#\#}$P<0.001 *vs.* TCS. GSDMD, gasdermin-D; DAPI, 4',6-diamidino-2-phenylindole; TCS, trichosanthin; NSA, necrosulfonamide.

NSA, an inhibitor of pyroptosis, effectively alleviated the inhibitory effect of TCS on the viability of A549 cells.

TCS is a single-chain ribosome-inactivating protein with a molecular weight of 27 kDa composed of 247 amino acid residues. In previous years, an increasing number of studies have revealed that TCS can significantly reduce the growth of a variety of tumors, including lung, colon, breast, and cervical cancer and has no effect on normal somatic cells, such as human peripheral blood lymphocytes (21). It is worth noting that the occurrence of tumors is closely related to apoptosis. TCS exerts its antitumor effect by activating different apoptotic pathways. Zhu *et al.* (22) reported that TCS could activate caspase-3 to induce apoptosis of lymphoma cells and suppress tumor activity. Kang *et al.* (23) demonstrated that TCS significantly increased the ratio of Bax/Bcl-2 to induce apoptosis and then inhibited the progression of nasopharyngeal carcinoma. In NSCLC, only one study showed that TCS could enhance the inhibitory effect of chemotherapeutic drugs on NSCLC cell activity by inhibiting the PI3K/AKT pathway (17). Generally speaking, there are still few studies on the role of TCS in NSCLC. In the present study, the effects of different concentrations of TCS (10, 20, and 40 μg/mL) on the viability, proliferation, migration, and invasion of A549 cells were determined via

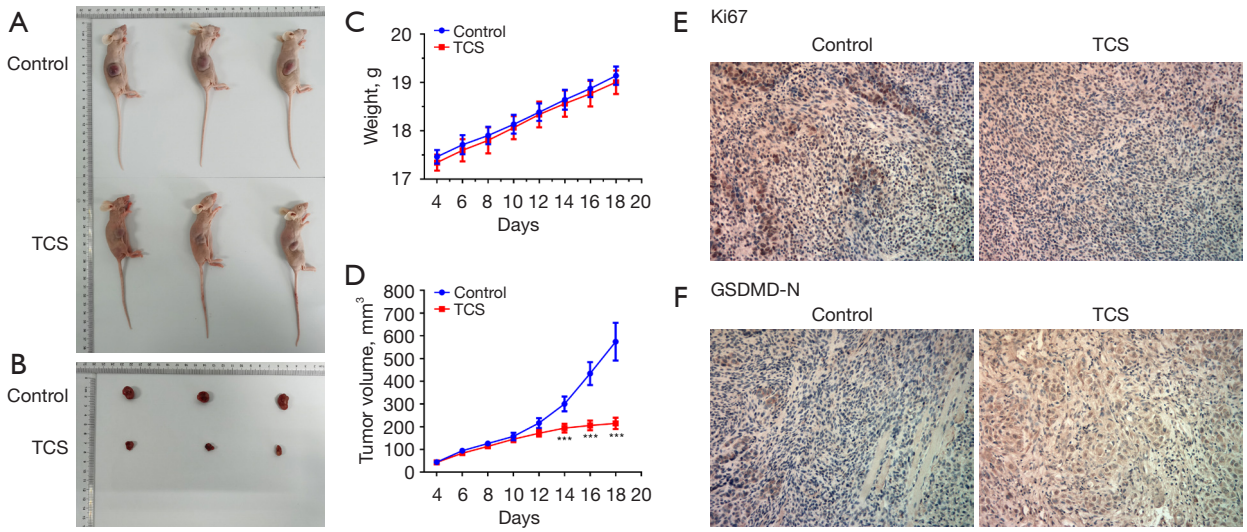

Figure 4 TCS inhibits the growth of tumor cells in mice. (A,B) The inhibition effects of TCS on tumor growth in an NSCLC mouse model. (C) The effect of treatment on mouse weight is assessed every 2 days. (D) The effect of treatment on tumor volume is assessed every 2 days. (E) Immunohistochemical staining detects Ki67 expression in the tumor tissues. Original magnification 200×. (F) Immunohistochemical staining detects GSDMD-N expression in the tumor tissues. Original magnification 200×. ***P<0.001 *vs.* control. TCS, trichosanthin; GSDMD, gasdermin-D; NSCLC, non-small cell lung cancer

CCK-8, colony formation, wound healing, and Transwell assays, respectively. TCS significantly inhibited the proliferation, migration, and invasion of A549 cells in a concentration-dependent manner. When the concentration of TCS was 40 μg/mL, the inhibitory activity of TCS on A549 cells was highest.

Pyroptosis is a newly discovered type of programmed cell death that differs from apoptosis. The occurrence of apoptosis is mainly due to the spontaneous and orderly cell death regulated by genes to maintain the stability of the internal environment (24). Pyroptosis is an inflammatory programmed death dependent on caspase-1, caspase-4, caspase-11, and GSDMD proteins and plays a key role in innate immunity (25-27). The study of apoptosis in tumors is common enough, but the relationship between pyroptosis and the occurrence and development of tumors remains to be further explored. In colorectal cancer, LXR receptor agonists can inhibit tumor progression by inducing the NLRP3 inflammasome assembly to activate caspase-1 (28). In gastric cancer, GSDMD silencing can inhibit the proliferation of gastric cancer cells by promoting pyroptosis via regulating cell cycle-related proteins (29). In lung cancer, GSDMD silencing has been found to significantly suppress the growth of NSCLC cells (30). Of note, resveratrol has been demonstrated to suppress NLRP3 progression by activating pyroptosis and inhibiting NSCLC inflammasome activation (31). However, whether TCS inhibits the progress of NSCLC by promoting pyroptosis has not yet been studied. In the present study, TCS significantly increased the expression of GSDMD-N, caspase-1, NLRP3, and ROS in a concentration-dependent manner, suggesting that the inhibitory effect of TCS on the progression of NSCLC may be associated with pyroptosis. In addition, the pyroptosis inhibitor NSA reduced the inhibitory effect of TCS on the proliferation, migration, and invasion of A549 cells. Meanwhile, the results of our *in vivo* experiments showed that TCS effectively suppressed the growth of tumors in mice and increased the expression of GSDMD-N in tumor tissues. Thus, we can consider that TCS may promote the process of pyroptosis to play the suppressive role in NSCLC. However, there are several limitations to this study. According to our results, TCS may directly regulate cell proliferation in addition to cell pyroptosis, and the inhibition of TCS on cell proliferation may not necessarily depend on activation of cell pyroptosis, which needs to be verified by further experiments. In this study, we preliminarily studied the effects of TCS on pyroptosis in NSCLC cells, but we have not studied the genetic mutation variation landscape of pyroptosis-related genes in NSCLC. In addition, we mainly detected the

relevant indicators involved in cell proliferation, metastasis, and pyroptosis in this work but did not investigate the effects of TCS on signaling pathways in NSCLC. The relationship between TCS and pyroptosis-related pathways and the pyroptosis-related genetic mutation will be researched in further study.

In conclusion, TCS reduced the proliferation, migration, and invasion of NSCLC cells by activating pyroptosis. This study further elucidates the mechanism underlying the anti-tumor effects of TCS to offer a new perspective on the diagnosis and treatment of NSCLC.

Acknowledgments

Funding: This study was sponsored by the Key Scientific Research Projects of the Hubei Education Department (grant No. D20181201) and Yunnan Provincial Department of Science and Technology-Kunming Medical University Joint Special Project on Applied Basic Research (grant No. 202001AY070001-290).

Footnote

Reporting Checklist: The authors have completed the ARRIVE reporting checklist. Available at https://jtd.amegroups.com/article/view/10.21037/jtd-22-282/rc

Data Sharing Statement: Available at https://jtd.amegroups.com/article/view/10.21037/jtd-22-282/dss

Conflicts of Interest: All authors have completed the ICMJE uniform disclosure form (available at https://jtd.amegroups.com/article/view/10.21037/jtd-22-282/coif). The authors have no conflicts of interest to declare.

Ethical Statement: The authors are accountable for all aspects of the work in ensuring that questions related to the accuracy or integrity of any part of the work are appropriately investigated and resolved. The present study was performed under a project license (No. YYLH017) granted by the Animal Care and Use Committee of The First People's Hospital of Yunnan Province (Kunming, China) and conducted in accordance with Chinese legislation regarding animal experiments.

References

1. Ferlay J, Soerjomataram I, Dikshit R, et al. Cancer incidence and mortality worldwide: sources, methods and major patterns in GLOBOCAN 2012. Int J Cancer 2015;136:E359-86.
2. Sève P, Reiman T, Dumontet C. The role of betaIII tubulin in predicting chemoresistance in non-small cell lung cancer. Lung Cancer 2010;67:136-43.
3. Raungrut P, Wongkotsila A, Lirdprapamongkol K, et al. Prognostic significance of 14-3-3γ overexpression in advanced non-small cell lung cancer. Asian Pac J Cancer Prev 2014;15:3513-8.
4. Shen T, Yang L, Zhang Z, et al. KIF20A Affects the Prognosis of Bladder Cancer by Promoting the Proliferation and Metastasis of Bladder Cancer Cells. Dis Markers 2019;2019:4863182.
5. Cagney DN, Martin AM, Catalano PJ, et al. Incidence and prognosis of patients with brain metastases at diagnosis of systemic malignancy: a population-based study. Neuro Oncol 2017;19:1511-21.
6. Zhang W, Zhang B, Vu T, et al. Molecular characterization of pro-metastatic functions of β4-integrin in colorectal cancer. Oncotarget 2017;8:92333-45.
7. Goldar S, Khaniani MS, Derakhshan SM, et al. Molecular mechanisms of apoptosis and roles in cancer development and treatment. Asian Pac J Cancer Prev 2015;16:2129-44.
8. Zhang QL, Yang JJ, Zhang HS. Carvedilol (CAR) combined with carnosic acid (CAA) attenuates doxorubicin-induced cardiotoxicity by suppressing excessive oxidative stress, inflammation, apoptosis and autophagy. Biomed Pharmacother 2019;109:71-83.
9. Karki R, Kanneganti TD. Diverging inflammasome signals in tumorigenesis and potential targeting. Nat Rev Cancer 2019;19:197-214.
10. Wang F, Zhang W, Wu T, et al. Reduced interleukin-38 in non-small cell lung cancer is associated with tumour progression. Open Biol 2018;8:180132.
11. Hu B, Yang XR, Xu Y, et al. Systemic immune-inflammation index predicts prognosis of patients after curative resection for hepatocellular carcinoma. Clin

Cancer Res 2014;20:6212-22.
12. Shaw PC, Chan WL, Yeung HW, et al. Minireview: trichosanthin--a protein with multiple pharmacological properties. Life Sci 1994;55:253-62.
13. Zhu C, Zhang C, Cui X, et al. Trichosanthin inhibits cervical cancer by regulating oxidative stress-induced apoptosis. Bioengineered 2021;12:2779-90.
14. Fang EF, Zhang CZ, Zhang L, et al. Trichosanthin inhibits breast cancer cell proliferation in both cell lines and nude mice by promotion of apoptosis. PLoS One 2012;7:e41592.
15. Zhang C, Gong Y, Ma H, et al. Reactive oxygen species involved in trichosanthin-induced apoptosis of human choriocarcinoma cells. Biochem J 2001;355:653-61.
16. Wei B, Huang Q, Huang S, et al. Trichosanthin-induced autophagy in gastric cancer cell MKN-45 is dependent on reactive oxygen species (ROS) and NF-κB/p53 pathway. J Pharmacol Sci 2016;131:77-83.
17. Tuya N, Wang Y, Tong L, et al. Trichosanthin enhances the antitumor effect of gemcitabine in non-small cell lung cancer via inhibition of the PI3K/AKT pathway. Exp Ther Med 2017;14:5767-72.
18. You C, Sun Y, Zhang S, et al. Trichosanthin enhances sensitivity of non-small cell lung cancer (NSCLC) TRAIL-resistance cells. Int J Biol Sci 2018;14:217-27.
19. Wu X, Chung VCH, Lu P, et al. Chinese Herbal Medicine for Improving Quality of Life Among Nonsmall Cell Lung Cancer Patients: Overview of Systematic Reviews and Network Meta-Analysis. Medicine (Baltimore) 2016;95:e2410.
20. Ye X, Ng CC, Wong JH, et al. Ribosome-inactivating Proteins from Root Tubers and Seeds of Trichosan-thes kirilowii and Other Trichosanthes Species. Protein Pept Lett 2016;23:699-706.
21. Sha O, Niu J, Ng TB, et al. Anti-tumor action of trichosanthin, a type 1 ribosome-inactivating protein, employed in traditional Chinese medicine: a mini review. Cancer Chemother Pharmacol 2013;71:1387-93.
22. Zhu Y, Sun Y, Cai Y, et al. Trichosanthin reduces the viability of SU-DHL-2 cells via the activation of the extrinsic and intrinsic apoptotic pathways. Mol Med Rep 2016;13:403-11.
23. Kang M, Ou H, Wang R, et al. Effect of trichosanthin on apoptosis and telomerase activity of nasopharyngeal carcinomas in nude mice. J BUON 2013;18:675-82.
24. Fink SL, Cookson BT. Apoptosis, pyroptosis, and necrosis: mechanistic description of dead and dying eukaryotic cells. Infect Immun 2005;73:1907-16.
25. Petrilli V. The multifaceted roles of inflammasome proteins in cancer. Curr Opin Oncol 2017;29:35-40.
26. Jiménez Fernández D, Lamkanfi M. Inflammatory caspases: key regulators of inflammation and cell death. Biol Chem 2015;396:193-203.
27. Kayagaki N, Stowe IB, Lee BL, et al. Caspase-11 cleaves gasdermin D for non-canonical inflammasome signalling. Nature 2015;526:666-71.
28. Derangère V, Chevriaux A, Courtaut F, et al. Liver X receptor β activation induces pyroptosis of human and murine colon cancer cells. Cell Death Differ 2014;21:1914-24.
29. Wang WJ, Chen D, Jiang MZ, et al. Downregulation of gasdermin D promotes gastric cancer proliferation by regulating cell cycle-related proteins. J Dig Dis 2018;19:74-83.
30. Gao J, Qiu X, Xi G, et al. Downregulation of GSDMD attenuates tumor proliferation via the intrinsic mitochondrial apoptotic pathway and inhibition of EGFR/Akt signaling and predicts a good prognosis in non-small cell lung cancer. Oncol Rep 2018;40:1971-84.
31. Zou J, Yang Y, Yang Y, et al. Polydatin suppresses proliferation and metastasis of non-small cell lung cancer cells by inhibiting NLRP3 inflammasome activation via NF-κB pathway. Biomed Pharmacother 2018;108:130-6.

(English Language Editor: D. Fitzgerald)

Cite this article as: Tan Y, Xiang J, Huang Z, Wang L, Huang Y. Trichosanthin inhibits cell growth and metastasis by promoting pyroptosis in non-small cell lung cancer. J Thorac Dis 2022;14(4):1193-1202. doi: 10.21037/jtd-22-282